Cancer Management and Research

Elevate Series

Open Access Full Text Article

ORIGINAL RESEARCH

Serum tRF5-23-GlyTCC-2 Functions as a Tumor Suppressor and Novel Biomarker for Colorectal Cancer

Xinhui Lv[1,2], Hui Dai[1,2], Yu Wu[1,2], Jiyuan Yang[1,2], Guihua Wang[1,2], Xudong Wang[1,2]

[1]Department of Laboratory Medicine, Affiliated Hospital of Nantong University, Nantong, Jiangsu, People's Republic of China; [2]Medical School of Nantong University, Nantong, Jiangsu, People's Republic of China

Correspondence: Xudong Wang, Department of Laboratory Medicine, Affiliated Hospital of Nantong University, Medical School of Nantong University, Nantong, Jiangsu, 226001, People's Republic of China, Tel +86-13951318000, Email wangxudong88@hotmail.com

Background: Transfer RNA-derived small RNAs (tsRNAs) are a recently discovered class of non-coding RNAs with aberrant expression in various cancers. Substantial evidence implicates tsRNAs in the initiation and progression of colorectal cancer (CRC). This study aimed to investigate the diagnostic and prognostic potential of a specific tsRNA, tRF5-23-GlyTCC-2, in CRC.

Methods: We identified tRF5-23-GlyTCC-2 via high-throughput RNA sequencing and validated its expression using qRT-PCR. Associations between tRF5-23-GlyTCC-2 expression, clinicopathological features, and patient survival were assessed with Chi-square and Kaplan-Meier analyses. Its diagnostic performance was evaluated by ROC curve analysis. Functional roles in CRC were examined using colony formation assays and xenograft mouse models.

Results: Expression of tRF5-23-GlyTCC-2 was significantly downregulated in CRC tissues ($P = 0.0009$) and serum ($P < 0.0001$) compared to controls. It effectively discriminated CRC patients from healthy individuals and those with colorectal polyps, and served as a strong predictor of poor prognosis. Low tRF5-23-GlyTCC-2 levels were correlated with advanced invasion, metastasis ($P = 0.0153$), and poor prognosis ($P = 0.004$). ROC analysis demonstrated its superior diagnostic accuracy over traditional biomarkers (AUC = 0.8628), and its combination with CEA further improved the diagnostic performance (AUC = 0.9077). Both in vitro colony formation assays and in vivo xenograft models confirmed its tumor-suppressive function by inhibiting tumor growth and progression.

Conclusion: Serum tRF5-23-GlyTCC-2 exhibits high diagnostic accuracy, and its combination with CEA achieves superior sensitivity (84%), highlighting its potential as a powerful non-invasive biomarker to improve CRC detection and prognosis prediction.

Keywords: colorectal cancer, tsRNA, biomarker, carcinostasis, diagnosis

Introduction

Colorectal cancer (CRC) retains its status as the third most prevalent cancer globally, contributing significantly to morbidity and mortality, which persist as challenges to healthcare systems worldwide.[1–3] Despite the promise shown by therapeutic advancements, including immunotherapy and molecularly targeted therapies, the 5-year survival rates remain less than optimal, standing at 63% in Western populations and 56.9% in China. This highlights the critical need for improved diagnostic biomarkers to facilitate early intervention.[4–6] Current clinical biomarkers such as CEA, CA19-9, and CA72-4 demonstrate limited sensitivity and specificity for early-stage detection. Their suboptimal performance, particularly in detecting early-stage disease and precancerous lesions, underscores the pressing clinical need for more robust non-invasive biomarkers. This urgent demand continues to drive intensive research into novel molecular indicators with enhanced diagnostic precision and therapeutic relevance.[7–9] The focus has increasingly shifted towards circulating biomarkers, measured in serum or plasma, due to their non-invasive nature which enables facile longitudinal monitoring and greater potential for clinical translation compared to tissue-based assays.

Emerging insights into cancer biology have revealed the critical regulatory functions of non-coding RNAs, particularly transfer RNA-derived small RNAs (tsRNAs), which constitute a conserved class of non-coding RNAs produced via enzymatic processing of precursor or mature tRNAs.[10–12] These molecules are broadly categorized into tRNA-derived fragments (tRFs) and tRNA half-fragments (tiRNAs), with tRFs further subdivided into five distinct isoforms (i-tRF, tRF-1-5) and tiRNAs classified as

Received: 16 May 2025
Accepted: 14 October 2025
Published: 27 October 2025

Graphical Abstract

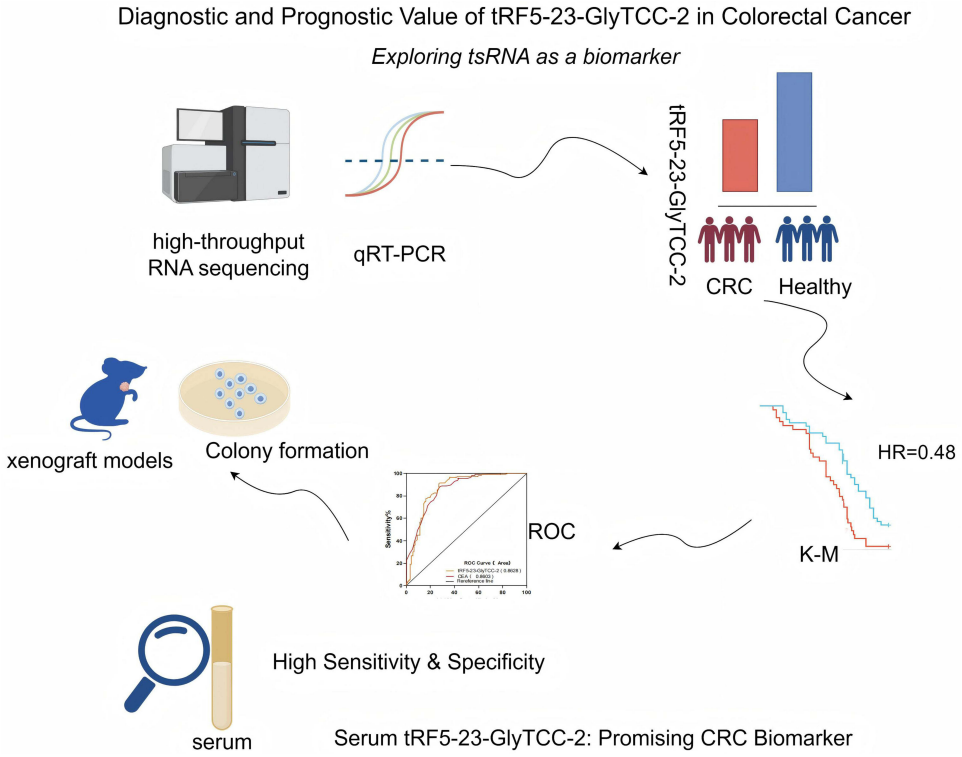

5′- or 3′-tiRNAs.[13] Functionally, tsRNAs regulate essential cellular processes including proliferation, apoptosis, and metabolic reprogramming through mechanisms such as ribosomal subunit binding for translation inhibition.[11,14] For tumor-suppressive tsRNAs, their consistent downregulation across tumors provides a stable and clinically actionable signal, making them particularly attractive candidates for biomarker development.

The tumorigenic potential of specific tsRNAs has been increasingly documented across malignancies.[15] In CRC pathogenesis, 5'tiRNA-His-GTG has been demonstrated to facilitate oncogenic progression through LARS2-mediated modulation of the Hippo pathway,[16] whereas tsRNA-GlyGCC promotes chemoresistance by manipulating the SPIB/JAK1/STAT6 signaling axis.[17] Parallel investigations in pancreatic cancer revealed tRF-Leu-AAG's role in enhancing metastatic potential,[18] whereas tRF-19-3L7L73JD exhibits tumor-suppressive properties by regulating the cell cycle regulation in other systems.[19] These findings position tsRNAs as both mechanistic mediators and potential diagnostic tools, with clinical studies identifying serum tsRNAs like tiRNA-Phe-GAA-003 and tRF-Arg-CCT-017 as promising biomarkers in breast cancer,[20] and tRF-Pro-AGG-004 and tRF-Leu-CAG-002 in pancreatic cancer.[21] In non-small cell lung cancer, tRF-Leu-CAG is upregulated, and serum tRF-17-WS7K092 has been identified as a dynamic surveillance marker in gastric cancer.[22,23] Similarly, serum tsRNA-ValTAC-41 has been implicated as a biomarker for pancreatic ductal adenocarcinoma.[24] However, the field still lacks well-validated circulating tsRNAs that offer combined diagnostic and prognostic value for CRC, particularly those capable of distinguishing malignant cancer from precancerous adenomas.

Among the various tsRNAs, those derived from glycine tRNA (Gly-tRNA) have garnered increasing interest for their roles in cellular stress response and tumorigenesis.[25,26] The fragment tRF5-23-GlyTCC-2, an internal tRNA fragment (i-tRF) originating from the 5′ end of GlyTCC tRNA on chromosome 6, is a less explored member of this family that may possess unique mechanistic properties. Preliminary evidence from other cancer types suggests that Gly-tRNA-derived tsRNAs can influence key oncogenic pathways,[17,27] leading us to hypothesize that tRF5-23-GlyTCC-2 could

function as both a tumor suppressor and a novel biomarker in CRC. However, its specific expression pattern, functional role, and clinical relevance in colorectal cancer remain entirely unknown. Given the urgent need for reliable CRC biomarkers and the emerging prognostic potential of tsRNAs, this study aims to comprehensively investigate its expression, clinical significance, and biological function in colorectal cancer.

Materials And Methods

Clinical Samples

From September 2018 to June 2021, a total of 313 participants at the Affiliated Hospital of Nantong University contributed serum samples. The inclusion criteria for CRC patients were: (1) histopathologically confirmed primary CRC; (2) no prior history of anticancer therapy; (3) availability of complete clinical and follow-up data. Patients with other malignant tumors, severe infectious diseases, or autoimmune disorders were excluded from the study.

This group comprised 122 individuals with colorectal cancer (CRC), 71 patients suffering from colon polyps, and 120 healthy people undergoing regular medical examinations. All CRC patients were diagnosed through histopathology and had not undergone any preoperative therapies. Blood samples were centrifuged at 3000 rpm for 10 minutes at 4°C to separate serum, which was then aliquoted and immediately stored at −80°C to prevent RNA degradation.

In addition, a careful collection of 32 pairs of colorectal cancer (CRC) tissues and their adjacent non-cancerous tissues, verified by the pathology department, was conducted. These biological samples were swiftly stored at −80°C to maintain their integrity for future analysis. The process of collecting clinical samples was carried out only after obtaining informed consent from all participants. Notably, all research endeavors involving human subjects underwent rigorous review and received formal approval from the Ethics Committees of the Affiliated Hospital of Nantong University (Approval Number: 2019-L053).

Patient Follow-up and Survival DataFor the survival analysis, all 122 enrolled CRC patients were actively monitored post-operatively. The follow-up process was conducted through regular outpatient visits and telephone interviews. Overall survival (OS) was defined as the time from the date of surgical intervention to the date of death from any cause or the last known follow-up. The median duration of follow-up for the cohort was 36 months (range, 4 to 36 months). By the end of the follow-up period, 65 deaths were recorded. Clinical data, including demographic information, tumor-node-metastasis (TNM) stage, and survival status, were meticulously extracted from the hospital's electronic medical record system. The inclusion criteria for participants in the survival analysis were: (1) pathologically confirmed primary CRC; (2) availability of complete clinical and follow-up data; and (3) having undergone curative-intent surgery.

Cell Culture

Four colorectal cancer cell lines—DLD1, HCT116, SW620, and SW1116—along with a normal intestinal epithelial cell line (NCM460), were sourced from the Cell Bank of the Chinese Academy of Sciences in Shanghai, China. Each cell line was validated through STR genotyping, with the most recent authentication taking place on September 9, 2021. All experiments were performed using cells between passages 5 and 20 to ensure phenotypic stability and reproducibility. For optimal growth conditions, the cells were cultivated in an incubator maintained at 37°C with a 5% CO_2 atmosphere. The choice of culture media included Dulbecco's Modified Eagle Medium (DMEM) and RPMI-1640 medium (5A), both enriched with 10% fetal bovine serum (FBS) and 1% penicillin-streptomycin.

RNA Extraction

Total RNA was extracted from both tissue samples and cultured cells utilizing TRIzol reagent (Invitrogen). Serum RNA was isolated using the Blood Total RNA Rapid Extraction Kit from BioTeke, following the protocol outlined by the manufacturer for centrifugal column extraction.

cDNA Synthesis and Quantitative Real-Time PCR (qRT-PCR)

Initially, complementary DNA (cDNA) was synthesized through reverse transcription reactions conducted at a temperature of 42°C for a duration of 60 minutes, followed by a 5-minute enzyme inactivation step at 70°C, as per

the protocols provided by Biosharp. Subsequently, quantitative reverse transcription polymerase chain reaction (qRT-PCR) was employed to assess RNA expression levels. The ChamQ Universal SYBR qPCR Master Mix was utilized for this procedure. The total reaction volume was 20 μL, comprising 10 μL of the qPCR Master Mix, 1 μL each of forward and reverse primers, 3 μL of enzyme-free water, and 5 μL of cDNA. The primers were specifically designed to target U6 (RUN6B) and tRF5-23-GlyTCC-2 (RIBOBIO). The relative expression levels were determined using the 2^−ΔΔCT method, with U6 serving as a quality control indicator.

Cell Transfection

Cells were seeded in 6-well plates and cultured until reaching 60–70% confluence to ensure optimal density for experiments. Conduct transient transfection utilizing the tRF5-23-GlyTCC-2 mimic or inhibitor. Besides, we used Lipofectamine 3000 (Thermo Fisher Scientific) to perform transfections following the manufacturer's instructions, including the use of corresponding negative controls (NCs) from Gene Pharma. Continue culturing for 24–48 hours after transfection, then begin functional experiments.

Clone Formation Assay

A total of 1×10^3 transfected cells were seeded into each well of 6-well plates to maintain a consistent, predetermined cell density for reliable experimental outcomes. The medium was replaced every four days for a total duration of 14 days to ensure optimal culture conditions and consistent cellular growth. Subsequently, cells were fixed with 4% paraformaldehyde (BioSharp) at ambient temperature, then stained with crystal violet and photographed for documentation.

Methodological Assessment

Room Temperature Stability and Freeze-Thaw Cycle Evaluation

The stability of tRF5-23-GlyTCC-2 in 20 pooled serum samples was investigated through a series of freeze-thaw cycles. These cycles ranged from 0 to 7 and involved alternating temperatures of −80°C and room temperature.Additionally, samples were kept at room temperature for various durations (0, 6, 12, 18, and 24 hours), and tRF5-23-GlyTCC-2 levels were measured at each time point.

Intra- and Inter-Batch Reproducibility

To ensure the reproducibility of the findings, the 20 pooled serum samples were divided into two groups, each consisting of 10 aliquots. One group was analyzed in a single batch, whereas the other group was examined over a period of 10 consecutive days, with a single sample being analyzed each day. The Ct values for tRF5-23-GlyTCC-2 and U6 were then utilized to compute the intra-batch and inter-batch coefficients of variation (CV), providing a measure of the variability within and between the batches.

Tumor xenograft In Nude Mice

To facilitate acclimatization and establish a stable physiological state, eight 4-week-old female BALB/c nude mice were obtained from the Experimental Animal Center of Nantong Medical College. These mice were then kept under controlled conditions for an additional four weeks. To create subcutaneous tumor models, SW1116 cells (2.5×10^6 per mouse) were injected into the axillary region of the nude mice using a precise and standardized technique to ensure uniformity. The mice were randomly divided into two groups: one receiving the ts agomir and the other receiving the nc agomir. Specifically, nine days post-implantation, either ts agomir or nc agomir (20 μg per mouse) was administered intratumorally at three-day intervals. Tumor growth was monitored by measuring length and width every three days using quantitative methods, which enabled the creation of growth curves. Following four injections, the mice were humanely euthanized using CO_2 asphyxia, in line with ethical guidelines. The excised tumors were weighed and preserved at −80°C for subsequent analysis.

Approval for this study was granted by the Animal Experiment Ethics Committee of Nantong University (Approval No. S20241126-026). All procedures were conducted in strict adherence to the ethical principles for animal research

outlined in the Basel Declaration and the guidelines set forth by the International Council for Laboratory Animal Science (ICLAS). Every effort was made to minimize the number of animals used and to alleviate their suffering.

Statistical Analysis

The data were meticulously analyzed utilizing SPSS software (version 26.0) and visually represented with GraphPad Prism (version 8.0), employing sophisticated statistical methods and graphical tools. To compare serum tRF5-23-GlyTCC-2 levels among different groups, a combination of one-way ANOVA and independent *t*-tests was employed to ascertain significant variations. The Chi-square test was utilized to determine if there was an association between tRF5-23-GlyTCC-2 levels and various patient characteristics, a common approach for such data analysis. To assess the discriminative capability of tRF5-23-GlyTCC-2 between groups, we employed ROC curve analysis. Additionally, Kaplan-Meier curves were used to examine patient survival durations. A p-value below 0.05 was considered statistically significant. This comprehensive statistical strategy enabled us to evaluate the associations and the diagnostic performance effectively.

Result

Screening of tsRNAs and Identification of tRF5-23-GlyTCC-2

To identify tsRNAs with differential expression in colorectal cancer (CRC) tissues, we conducted high-throughput sequencing on six pairs of CRC tissues and paired adjacent tissues. Through statistical analysis ($P < 0.05$ and log2 fold change < -1), we identified two tsRNAs that were significantly less abundant in CRC tissues: tRF5-23-GlyTCC-2 and tRF5-30-LysCTT-2.

In a larger cohort of 20 paired CRC tissue samples, reverse transcription quantitative polymerase chain reaction (RT-qPCR) validation revealed that tRF5-23-GlyTCC-2 expression was significantly reduced in CRC tissues when compared to adjacent normal tissues (Figure 1A). Additional quantitative RT-PCR (qRT-PCR) analysis of 32 CRC tissue samples further confirmed a significant reduction in tRF5-23-GlyTCC-2 expression in CRC tissues compared to matched paracarcinoma tissues ($P = 0.0009$) (Figure 1B).

Moreover, a substantial reduction in the levels of tRF5-23-GlyTCC-2 was detected in the serum of colorectal cancer (CRC) patients when compared to healthy controls ($P < 0.0001$), as demonstrated by the analysis of serum samples from both cohorts (Figure 1C). Importantly, a positive correlation was identified between the expression levels of tRF5-23-GlyTCC-2 in serum and those in the corresponding CRC tissues, indicating that patients with diminished serum expression levels also presented lower levels in the associated tumor tissues ($P < 0.0001$) (Figure 1D).

In addition to tissue and serum samples, we evaluated tRF5-23-GlyTCC-2 expression in CRC cell lines, including NCM460, DLD1, SW620, SW1116, and HCT116. The expression of tRF5-23-GlyTCC-2 was significantly downregulated in most CRC cell lines compared to the normal NCM460 cell line, although it was elevated in SW1116 (Figure 1E). Based on these findings, tRF5-23-GlyTCC-2 was prioritized for further study.

Establishment and Evaluation of the Detection Method for tRF5-23-GlyTCC-2

To describe the genomic architecture of tRF5-23-GlyTCC-2, we accessed the UCSC Genome Browser database (https://genome-asia.ucsc.edu/). The analysis revealed that tRF5-23-GlyTCC-2 originates from chromosome 6 (coordinates: 40500001–46,200,000), specifically spanning positions 42529286–42,529,308 (Supplementary Figure 1A). Using MINTbase v2.0 (https://cm.jefferson.edu/MINTbase/) and the tsRFun database (https://rna.sysu.edu.cn/tsRFun/cancer.php), we identified tRF5-23-GlyTCC-2 as an i-tRF (internal tRF) with a sequence of 5′-GCGTTGGTGGTATAGTGGTGAGC-3′, derived from tRNA-GlyTCC and measuring 23 nucleotides in length (Supplementary Figure 1B and C).

With the aim of evaluating tRF5-23-GlyTCC-2's potential as a novel biomarker for colorectal cancer (CRC) and its clinical applicability, we conducted a comprehensive assessment of the detection assay.The detection performance of tRF5-23-GlyTCC-2 in mixed serum samples was first evaluated by analyzing intra- and inter-assay variability. Results showed that the assay exhibited excellent reproducibility, with low coefficients of variation, confirming its precision (Table 1).

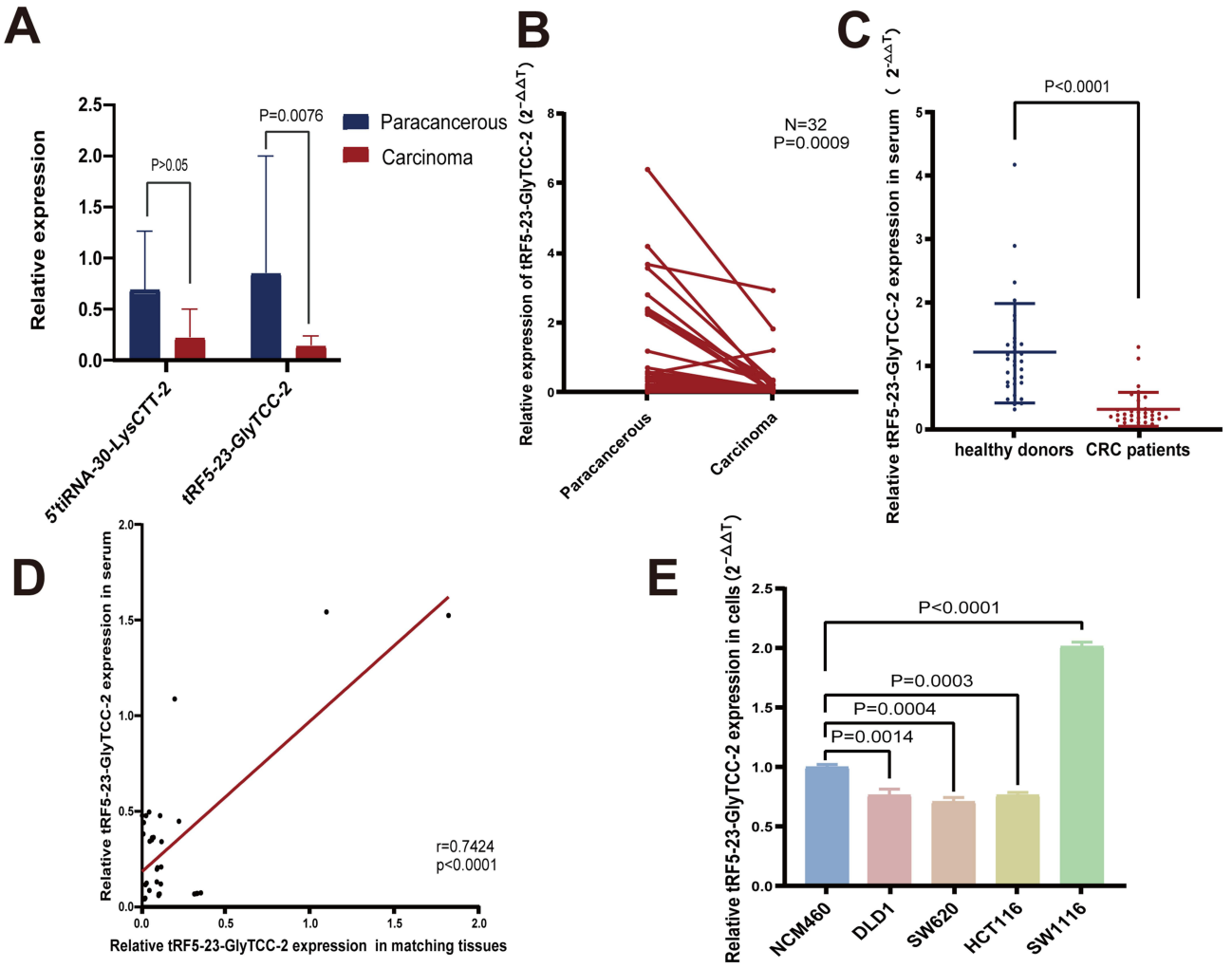

Figure 1 Screening of tsRNAs in patients with Colorectal Cancer (CRC). (**A**) Relative expression levels of two lowly expressed tsRNAs in 20 pairs of CRC tissues. (**B**) Expression levels of tRF5-23-GlyTCC-2 in 32 pairs of CRC tissues and their corresponding paracancerous tissues. (**C**) Correlation analysis of tRF5-23-GlyTCC-2 expression levels between 32 CRC tissues and their corresponding serum samples. (**D**) Expression levels of tRF5-23-GlyTCC-2 in serum samples from CRC patients (n=32) and healthy donors (n=32). (**E**) Expression levels of tRF5-23-GlyTCC-2 across different CRC cell lines.

Subsequently, to evaluate the stability of the assay, mixed serum samples were subjected to a range of conditions. The samples were divided into two groups, with one group maintained at room temperature for intervals of 0, 6, 12, 18, and 24 hours, while the other group underwent multiple freeze-thaw cycles at both room temperature and −80°C (specifically, 0, 1, 3, 5, and 10 cycles). Under these experimental conditions, no significant changes in the expression levels of tRF5-23-GlyTCC-2 were detected, thereby demonstrating its remarkable stability in serum samples (Figure 2A and B).

To further ensure the integrity and accuracy of the RT-qPCR products, we employed agarose gel electrophoresis. The results of the electrophoresis revealed distinct bands at around 80 bp (Figure 2C). Subsequent Sanger sequencing confirmed that the product contained the complete sequence of tRF5-23-GlyTCC-2, which was consistent with the

Table 1 The Intra-Assay CV and the Inter-Assay CV of tRF5-23-GlyTCC-2

	tRF5-23-GlyTCC-2	RNU6B
Intra-assay CV (%)	2.17	2.23
Inter-assay CV (%)	2.32	2.71

Abbreviation: CV, coefficient of variation.

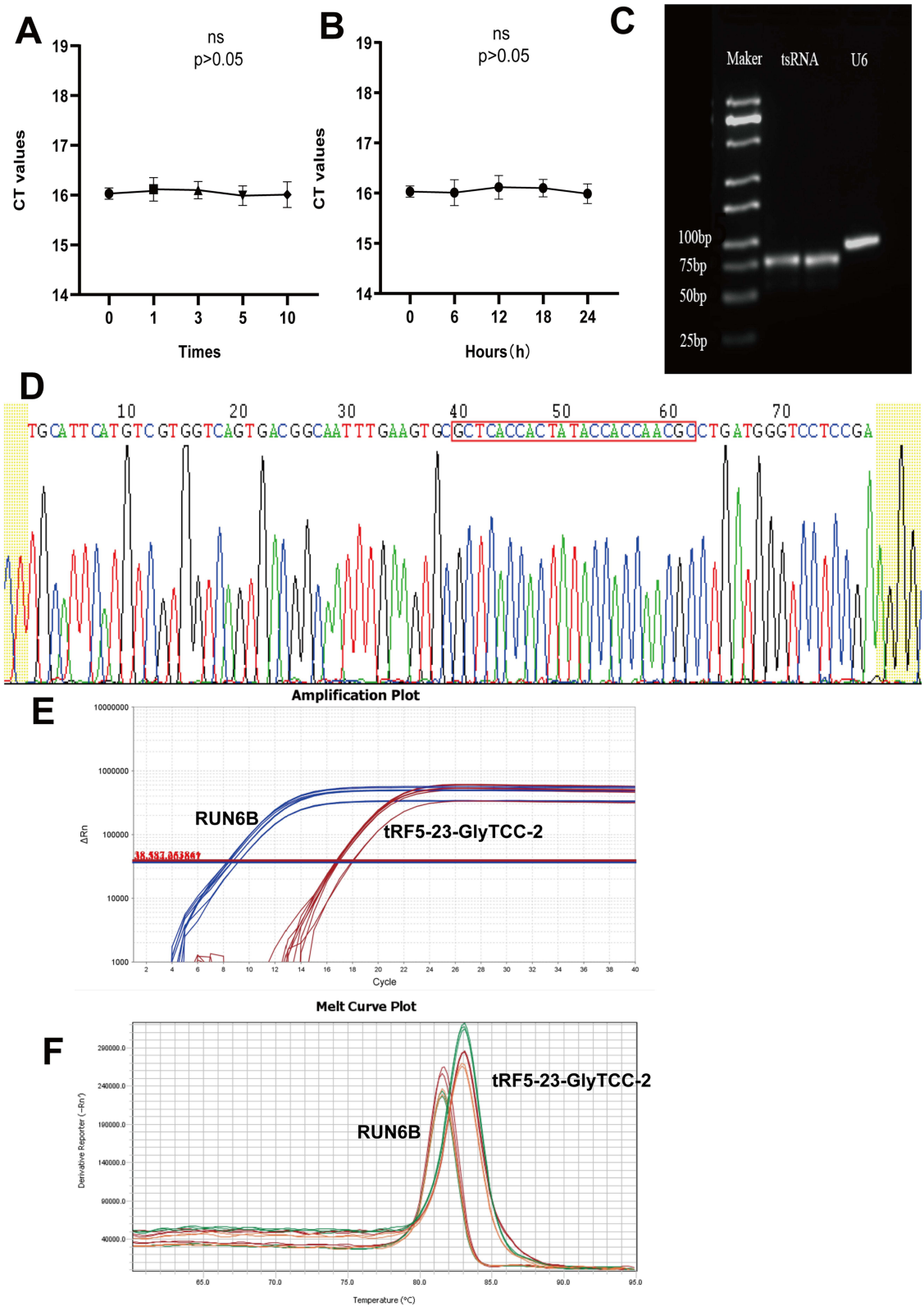

Figure 2 Establishment and evaluation of methods to detect tRF5-23-GlyTCC-2. (**A** and **B**) Stability assessment: Room temperature and repeated freeze-thaw experiments showed no significant changes in the expression levels of tRF5-23-GlyTCC-2. (ns, p>0.05) (**C**) Agarose gel electrophoresis confirmed the RT-qPCR product of tRF5-23-GlyTCC-2 as a single band of approximately 80 bp. The red box represents the sequence of tRF5-23-GlyTCC-2. (**D**) Sanger sequencing of the RT-qPCR product verified the presence of the full-length sequence of tRF5-23-GlyTCC-2. (**E**) Amplification curve analysis: Red lines indicate tRF5-23-GlyTCC-2, and blue lines represent RNU6B. (**F**) Melting curve analysis: Left lines represent RNU6B, and right lines correspond to tRF5-23-GlyTCC-2.

https://doi.org/10.2147/CMAR.S540752

sequence recorded in MINTbase v2.0 (Figure 2D). Additionally, the specificity of the method was established by observing a single-peak melting curve and a smoothed amplification curve (Figure 2E and F).

Low Expression of Serum tRF5-23-GlyTCC-2 Correlates with Poor Survival

To evaluate tRF5-23-GlyTCC-2 expression in colorectal cancer (CRC), we analyzed serum samples from 122 CRC patients, 71 colon polyp patients, and 120 healthy donors using qRT-PCR (Figure 3A). CRC patients exhibited significantly lower expression levels compared to both polyp patients (P=0.0005) and healthy controls (P<0.0001), while no significant difference was observed between polyp patients and controls (P=0.0798).

When stratifying CRC patients by median expression (0.219) into high- (n=61) and low-expression (n=61) groups, the low-expression group showed strong associations with clinicopathological features (Table 2), including advanced T stage (P=0.006), poor tumor differentiation (P=0.001), higher TNM stage (P=0.006), neurological/vascular invasion (P=0.018), and lymph node metastasis (P=0.011). Tumor size, age, gender, and C-erbB-2 status showed no significant correlations.

Subgroup analyses revealed progressive expression decline with disease severity. Compared to healthy controls, T3-T4 tumors showed lower expression than T1-T2 tumors (P=0.0002 vs P<0.0001), though inter-stage differences were non-significant (P=0.8447) (Figure 3B). TNM stage comparisons showed comparable levels between stages I–II and III–IV (P=0.9017), both being significantly lower than controls (P<0.0001) (Figure 3C). Notably, metastatic cases demonstrated reduced expression versus non-metastatic cases (P=0.0153) (Figure 3D), paralleling findings in neurological/vascular invasion (P=0.0425) (Figure 3E).

Postoperative monitoring of 57 CRC patients revealed significant tRF5-23-GlyTCC-2 elevation compared to preoperative levels (P<0.0001) (Figure 3F), reaching levels comparable to healthy controls (P=0.2424) (Figure 3G). Kaplan-Meier analysis confirmed that low preoperative expression predicted reduced overall survival (Figure 3H). These findings collectively establish serum tRF5-23-GlyTCC-2 as a potential dual biomarker for CRC prognosis and postoperative monitoring.

Combined Detection of Serum tRF5-23-GlyTCC-2 and CEA Improves Diagnostic Accuracy in CRC

To evaluate the diagnostic utility of tRF5-23-GlyTCC-2 in colorectal cancer (CRC), we compared its performance with conventional biomarkers (CEA, CA72-4, and CA19-9). Given that CA72-4 and CA19-9 showed notably inferior diagnostic effectiveness compared to CEA, our analysis concentrated on the joint assessment of tRF5-23-GlyTCC-2 and CEA.

The Receiver Operating Characteristic (ROC) curve analysis, which compared 122 CRC patients with 120 healthy donors, highlighted tRF5-23-GlyTCC-2's superior diagnostic capabilities. It achieved an Area Under the Curve (AUC) of 0.8628 (95% Confidence Interval: 0.8145–0.9112), marginally surpassing CEA's AUC of 0.8603 (95% CI: 0.8141–0.9065) (Figure 4A). Utilizing a cutoff value of 0.381 and a Youden index of 0.647, tRF5-23-GlyTCC-2 exhibited a sensitivity of 74% and a specificity of 92%, whereas CEA had a sensitivity of 70% and a specificity of 88%. Furthermore, tRF5-23-GlyTCC-2 outperformed CEA in overall accuracy (82%), positive predictive value (PPV: 90%), and negative predictive value (NPV: 77%), underscoring its potential as a reliable diagnostic marker (Table 3).

The integration of tRF5-23-GlyTCC-2 with CEA notably enhanced diagnostic discrimination, resulting in a combined Area Under the Curve (AUC) of 0.9077 (95% Confidence Interval: 0.8696–0.9459) and significantly increasing sensitivity to 90% (Figure 4B and Table 3).

Given the clinical challenge of distinguishing CRC from precancerous colorectal polyps, we further assessed tRF5-23-GlyTCC-2's discriminatory capacity. ROC analysis revealed an AUC of 0.7200 (95% CI: 0.6467–0.7934) for tRF5-23-GlyTCC-2, surpassing CEA's AUC of 0.6743 (95% CI: 0.5942–0.7543) (Figure 4C). At a cutoff of 0.3627 (Youden index=0.370), tRF5-23-GlyTCC-2 demonstrated superior sensitivity (72% vs 62%), specificity (65% vs 58%), accuracy (69% v 60%), PPV (78% vs 70%), and NPV (58% v 50%) compared to CEA (Table 4). Combinatorial analysis further enhanced diagnostic performance (AUC=0.7447, 95% CI: 0.6687–0.8207; sensitivity=84%) (Figure 4D and Table 4).

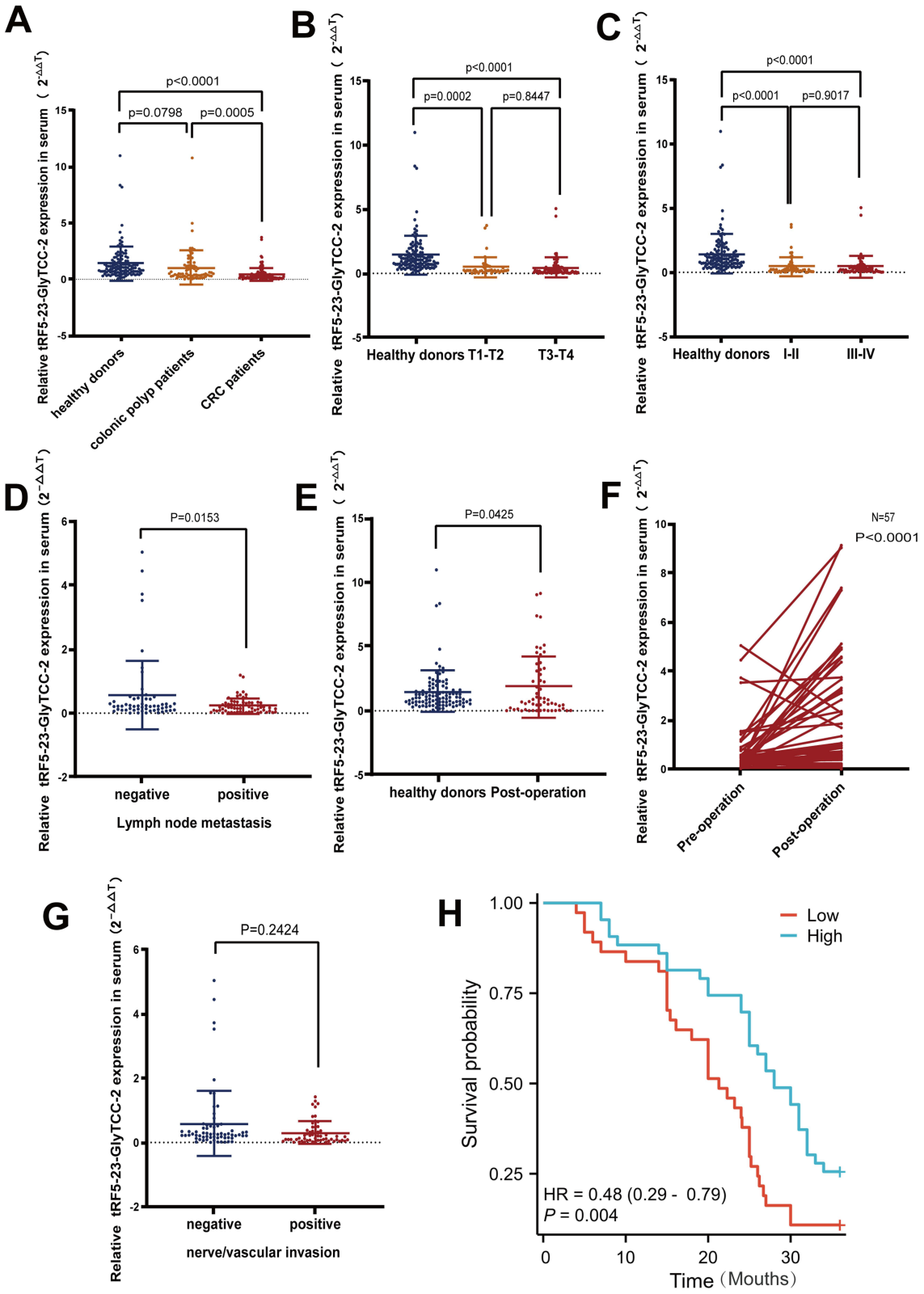

Figure 3 Diagnostic and prognostic value of serum tRF5-23-GlyTCC-2. (**A**) Serum expression levels of tRF5-23-GlyTCC-2 in colorectal cancer (CRC) patients (n=122), patients with colon polyps (n=71), and healthy donors (n=120). (**B**) Comparison of tRF5-23-GlyTCC-2 expression levels among CRC patients with varying depths of tumor invasion (T1–T2: n=49; T3–T4: n=73) and healthy donors (n=120). (**C**) Serum expression levels of tRF5-23-GlyTCC-2 in stage I–II CRC patients (n=53), stage III–IV patients (n=69), and healthy donors (n=120). (**D**) Differential expression levels of tRF5-23-GlyTCC-2 in CRC patients with (n=66) and without lymph node metastasis (n=56). (**E**) Expression levels of tRF5-23-GlyTCC-2 in CRC patients with (n=53) and without nerve/vascular invasion (n=69). (**F**) Serum tRF5-23-GlyTCC-2 levels in 57 CRC patients before and after surgical intervention. (**G**) Comparison of tRF5-23-GlyTCC-2 levels between postoperative CRC patients and healthy donors. (**H**) Kaplan-Meier survival curve illustrating the association between preoperative serum tRF5-23-GlyTCC-2 levels and CRC patient survival.

https://doi.org/10.2147/CMAR.S540752

Table 2 Clinicopathological Analysis of tRF5-23-GlyTCC-2

Parameter		No. of Patients	tRF5-23-GlyTCC-2		p value
			High (n=61)	Low (n=61)	
Sex	Male	63	29	34	0.365
	Female	59	32	27	
Age (year)	>60	82	44	38	0.247
	≤60	40	17	23	
Tumor size	>5	22	9	13	0.346
	≤5	100	52	48	
Differentiation grade	Well-moderate	89	53	36	0.001
	Poor	33	8	25	
T stage	T1-T2	49	32	17	0.006
	T3-T4	73	29	44	
Lymph node status	Positive	66	26	40	0.011
	Negative	56	35	21	
TNM stage	I–II	53	34	19	0.006
	III–IV	69	27	42	
Nerve/vascular-invasion	Positive	53	20	33	0.018
	Negative	69	41	28	
C-erbB-2	Positive	38	16	22	0.241
	Negative	84	45	39	

Notes: *p < 0.05; **p < 0.01; ***p < 0.001; ****p < 0.0001.
Abbreviation: TNM, tumor node metastasis.

Collectively, these findings establish tRF5-23-GlyTCC-2 as a reliable independent biomarker and demonstrate its synergistic diagnostic value when combined with CEA.

Overexpression of tRF5-23-GlyTCC-2 Suppresses Tumor Cell Growth in vivo and in vitro

The expression levels of tRF5-23-GlyTCC-2 were evaluated using qRT-PCR in various colorectal cancer (CRC) cell lines, including NCM460, DLD1, SW620, HCT116, and SW1116. The results revealed that tRF5-23-GlyTCC-2 was lowly expressed in SW620, HCT116 and DLD1 cells, while it was highly expressed in SW1116 cells (Figure 1E). Since we detected the transfection efficiency of tRF5-23-GlyTCC-2 inhibitor and mimics via RT-PCR, we excluded SW620 cells with poor transfection efficiency (Supplementary Figure 2A and B). To explore the functional implications of tRF5-23-GlyTCC-2 in CRC progression, we investigated its impact on cell proliferation by modulating its expression in HCT116, DLD1, and SW1116 cells. Transfection with a tRF5-23-GlyTCC-2 mimic significantly inhibited colony formation, whereas its inhibition promoted colony formation (Figure 5A), suggesting its tumor-suppressive role in CRC cells.

To further validate the in vivo effects of tRF5-23-GlyTCC-2, we established a xenograft tumor model by subcutaneously injecting 2.5 × 10^6 SW1116 cells into the right axillary region of nude mice. Nine days after inoculation, tumors were treated with NC agomir or tRF5-23-GlyTCC-2 agomir via intratumoral injection, administered once every three days for a total of four injections (Figure 5B). Tumor growth was monitored every three days, and tumors were harvested at the end of the experiment. The results demonstrated that tumors in the tRF5-23-GlyTCC-2 agomir group exhibited significantly reduced volume, weight, and growth rate compared to the control group (Figure 5C–F). These findings indicate that tRF5-23-GlyTCC-2 agomir can effectively inhibit tumor formation and growth in a xenograft model, further supporting its tumor-suppressive role in colorectal cancer progression.

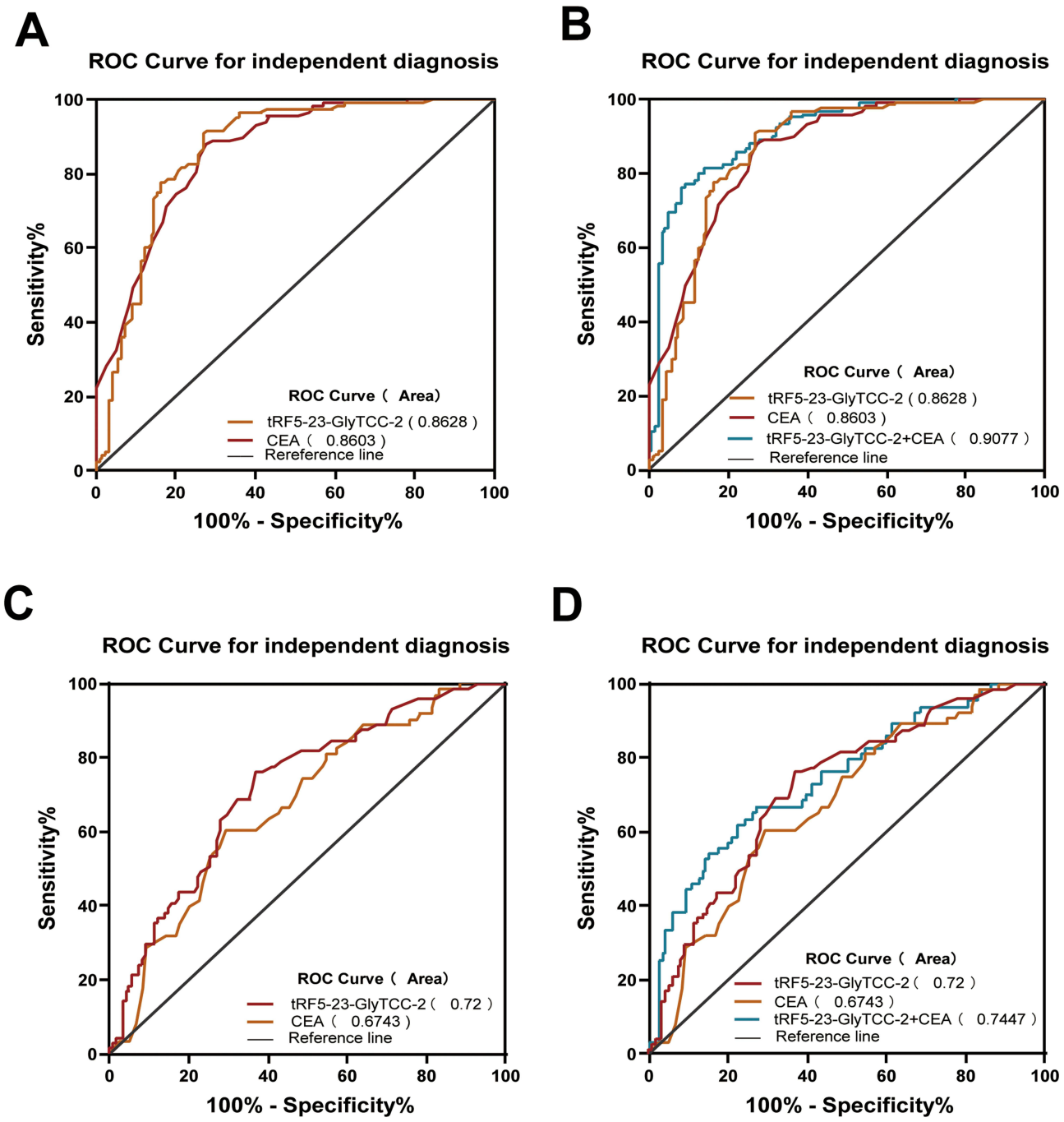

Figure 4 Serum tRF5-23-GlyTCC-2 combined with CEA enhances the adjunctive diagnosis of CRC. (**A**) ROC curves comparing the ability of tRF5-23-GlyTCC-2 and CEA to discriminate between colorectal cancer (CRC) patients (n=122) and healthy donors (n=120). (**B**) ROC curves comparing the ability of tRF5-23-GlyTCC-2, CEA, and their combination to discriminate between colorectal cancer (CRC) patients (n=122) and healthy donors (n=120). (**C**) ROC curves comparing the ability of tRF5-23-GlyTCC-2 and CEA to discriminate between CRC patients (n=122) and patients with colon polyps (n=71). (**D**) ROC curves comparing the ability of tRF5-23-GlyTCC-2, CEA, and their combination to discriminate between CRC patients (n=122) and patients with colon polyps (n=71).

Prediction of the Downstream Regulation Mechanism of tRF5-23-GlyTCC-2

To explore the underlying mechanisms of tRF5-23-GlyTCC-2 in colorectal cancer (CRC), the miRanda and TargetScan databases were utilized to identify potential target genes associated with tRF5-23-GlyTCC-2. As illustrated in Figure 6A, the 201 genes that were common to both databases were deemed the most likely targets of tRF5-23-GlyTCC-2. A subsequent analysis of KEGG pathways indicated significant enrichment in the MAPK signaling pathway, circadian

https://doi.org/10.2147/CMAR.S540752

Table 3 The Diagnostic Performance of tRF5-23-GlyTCC-2 and CEA in Differentiating CRC Patients From Healthy Donors

	SEN	SPE	ACCU	PPV	NPV
tRF5-23-GlyTCC-2	0.74(89/122)	0.92(110/120)	0.82(199/242)	0.90(89/99)	0.77(110/143)
CEA	0.70(86/122)	0.88(106/120)	0.79(192/242)	0.86(86/100)	0.75(106/142)
tRF5-23-GlyTCC-2+CEA	0.90(110/122)	0.70(84/120)	0.80(194/242)	0.75(110/146)	0.88(84/96)

Abbreviations: SEN, sensitivity; SPE, specificity; ACCU, overall accuracy; PPV, positive predictive value; NPV, negative predictive value.

Table 4 The Diagnostic Performance of tRF5-23-GlyTCC-2 and CEA in Differentiating CRC Patients From Colon Polyp Patients

	SEN	SPE	ACCU	PPV	NPV
tRF5-23-GlyTCC-2	0.72(88/122)	0.65(46/71)	0.69(134/193)	0.78(88/113)	0.58(46/80)
CEA	0.70(85/122)	0.61(43/71)	0.66(128/193)	0.75(85/113)	0.54(43/80)
tRF5-23-GlyTCC-2+CEA	0.84(102/122)	0.55(39/71)	0.73(141/193)	0.76(102/134)	0.66(39/59)

Abbreviations: SEN, sensitivity; SPE, specificity; ACCU, overall accuracy; PPV, positive predictive value; NPV, negative predictive value.

entrainment, and aldosterone synthesis and secretion (Figure 6B and C). Furthermore, the potential target genes exhibited significant enrichment in biological processes and regulation of potassium channel complexes, as determined by Gene Ontology (GO) functional enrichment analysis (Figure 6D). Nonetheless, the fundamental regulatory mechanisms of tRF5-23-GlyTCC-2 warrant further investigation.

Discussion

High-throughput sequencing technologies have catalyzed biomarker discovery through systematic gene expression profiling. Within this paradigm, non-coding RNAs (ncRNAs), including long non-coding RNAs (lncRNAs), microRNAs (miRNAs), and circular RNAs (circRNAs), have emerged as pivotal candidates for liquid biopsy applications.[28] Among these, transfer RNA-derived small RNAs (tsRNAs) have recently emerged as a novel diagnostic RNA subclass with great biomarker potential.[29] These tsRNAs, produced through tRNA processing, exhibit remarkable stability in various biofluids such as serum and are involved in a wide array of biological processes.[30]

Our identification of tRF5-23-GlyTCC-2 as a downregulated i-tRF in CRC aligns with the growing recognition of tsRNAs as key players in tumorigenesis. However, its specific role appears to be context-dependent. For instance, while our study identified tRF5-23-GlyTCC-2 as a tumor-suppressive tsRNAs in CRC, other studies have reported similar tumor-suppressive roles of tsRNAs in other cancers such as 5′-tiRNA-Gln inhibits HCC progression by repressing translation.[31] Conversely, numerous studies have also documented oncogenic tsRNAs that promote CRC progression, such as tRF-GlyGCC promotes CRC progression by regulating SPIB.[32] This dichotomy highlights the functional diversity of tsRNAs and underscores the importance of characterizing each individual fragment. The observation that tRF5-23-GlyTCC-2 is derived from tRNA-GlyTCC is particularly intriguing, as glycine has been implicated in cancer metabolism and proliferation. It is plausible that tsRNAs derived from specific tRNAs may participate in regulating metabolic pathways relevant to their cognate amino acids, a hypothesis that warrants future investigation.

These analyses identified tRF5-23-GlyTCC-2 as a significantly downregulated tsRNAs in CRC. Its consistent downregulation across clinical specimens and strong correlation with aggressive disease parameters such as lymph node metastasis, advanced TNM stage and poor survival firmly establish its role as both a potent tumor suppressor and a dual-purpose biomarker for CRC.

The clinical translational value of tRF5-23-GlyTCC-2 is underscored by its superior diagnostic and prognostic performance. It effectively distinguished CRC patients from healthy controls with high accuracy (AUC=0.8628; 74% sensitivity, 92% specificity), outperforming the conventional biomarker CEA. Most notably, it demonstrated a unique

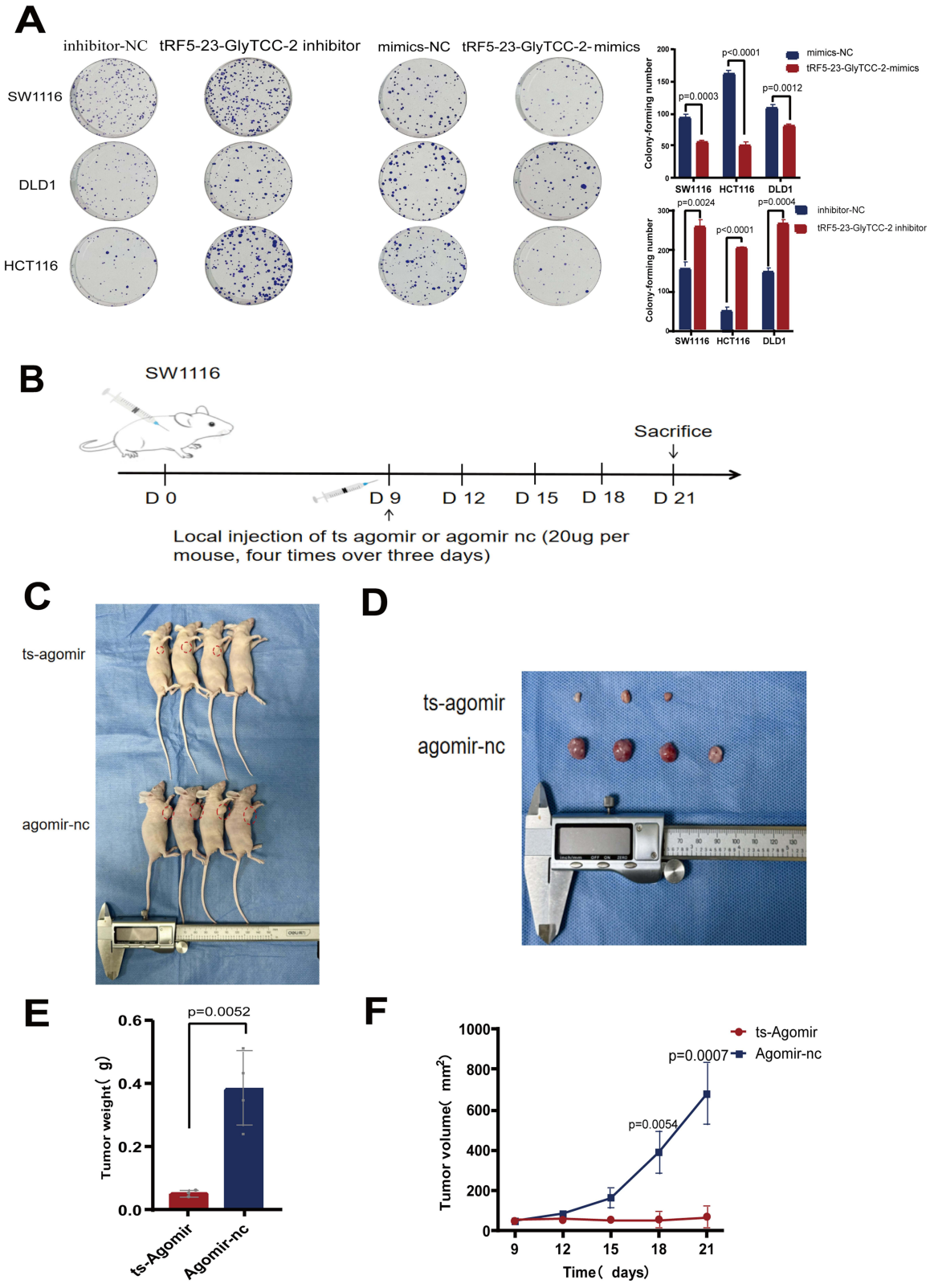

Figure 5 tRF5-23-GlyTCC-2 exhibits anti-cancer effects both in vivo and in vitro. (**A**) The impact of transfection with tRF5-23-GlyTCC-2 inhibitors and mimics on the proliferation of SW116, HCT116, and DLD1 cells was assessed through a cell colony formation experiment. (**B**) Animal experiment workflow diagram. (**C** and **D**) Establishment of CRC cell line xenograft tumor model in nude mice. (**E**) Tumor tissue weight in nude mice. (**F**) Tumor volume growth curve in nude mice.

https://doi.org/10.2147/CMAR.S540752

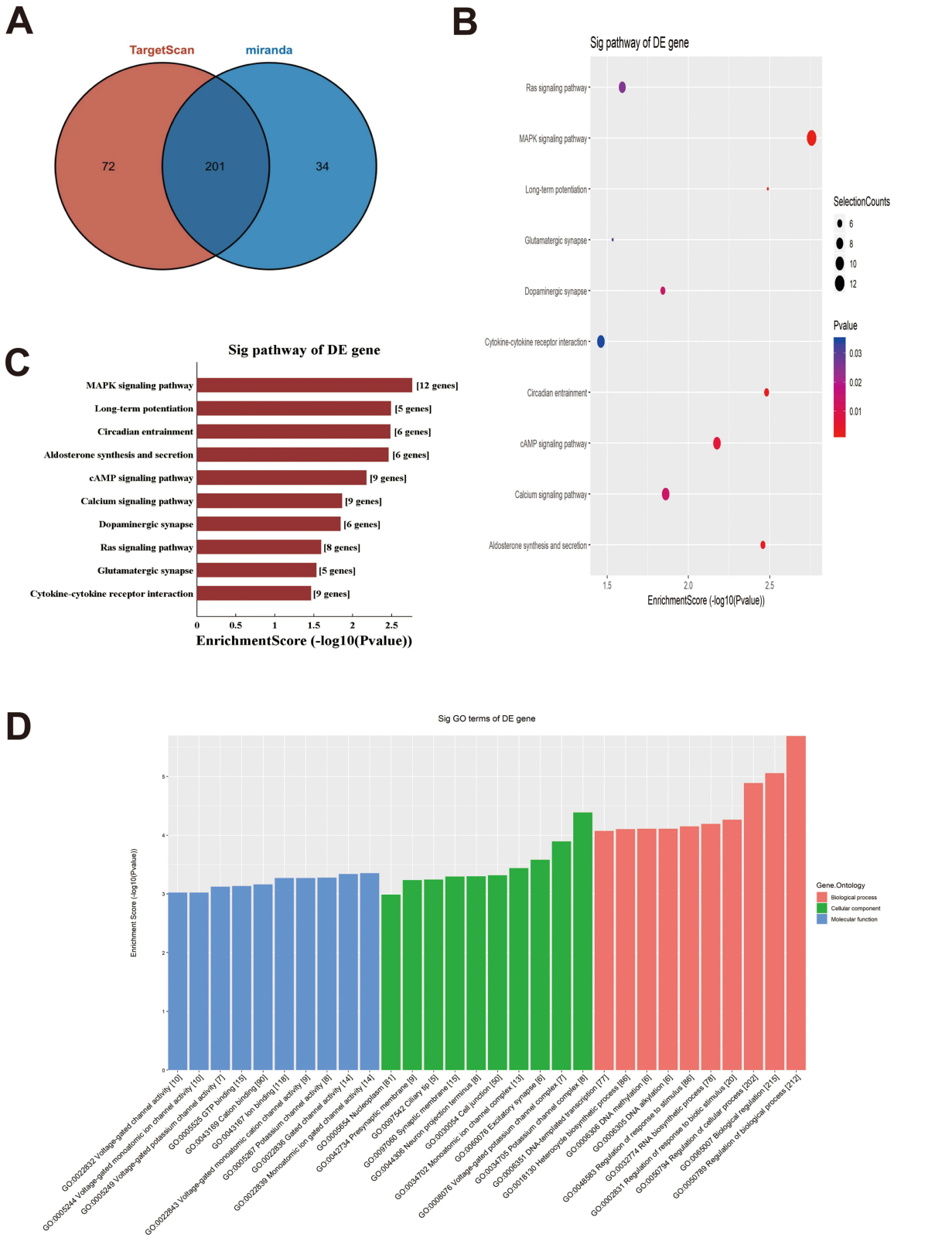

Figure 6 Prediction of the downstream regulation mechanism of tRF5-23-GlyTCC-2 (**A**) Venn diagram evaluating the overlapping genes predicted by the miRanda and TargetScan databases. (**B** and **C**) Kyoto Encyclopedia of Genes and Genomes (KEGG) pathway enrichment analysis of the potential target genes. The bar chart (**B**) and bubble chart (**C**) display the top significantly enriched pathways. The label "Sig pathway of DE gene" on the axes refers to "Significantly enriched pathways of differentially expressed genes" (the predicted target genes). The Rich Factor and P-value indicate the degree and statistical significance of the enrichment, respectively. (**D**) Gene Ontology (GO) functional enrichment analysis of the potential target genes. The bar chart shows the top significantly enriched terms across the three GO categories: Biological Process (BP), Molecular Function (MF), and Cellular Component (CC). The label "Sig Go terms of DE gene" on the axis refers to "Significantly enriched Gene Ontology terms of differentially expressed genes" (the predicted target genes). The Rich Factor and P-value indicate the degree and statistical significance of the enrichment, respectively.

ability to differentiate CRC from precancerous colon polyps (AUC=0.7200), a critical challenge in clinical practice where CEA performs poorly. While its standalone positive predictive value (78%) may limit individual use, our most significant finding reveals a powerful synergistic effect when combined with CEA, achieving exceptional diagnostic power (AUC=0.9077 vs healthy controls; 84% sensitivity vs polyps). This combinatorial approach leverages the strengths of both markers, offering a clinically actionable strategy that aligns with the growing trend toward multi-marker panels in precision oncology.

Beyond its diagnostic utility, our functional investigations provide compelling biological rationale for its tumor-suppressive role. The inhibition of CRC cell proliferation in vitro and significant attenuation of tumor growth in vivo upon tRF5-23-GlyTCC-2 restoration directly explain its consistent downregulation in aggressive clinical phenotypes. This functional evidence strongly supports its potential as a therapeutic target, suggesting that agomir-based strategies to restore its expression warrant further investigation. To explore its mechanistic underpinnings, our bioinformatic analysis revealed a significant enrichment of potential target genes in the MAPK signaling pathway, a well-established driver of CRC progression. While this data-driven hypothesis suggests tRF5-23-GlyTCC-2 may repress key oncogenic components within this pathway, this specific mechanistic link requires experimental validation through future studies identifying its direct binding partners and downstream targets.

Despite these promising findings, several limitations must be acknowledged. The single-center origin of our clinical cohort may affect the generalizability of our findings across diverse populations. Although our sample size was sufficient for initial discovery and validation, larger multi-center studies are essential to firmly establish its clinical utility. Furthermore, the precise molecular mechanism by which tRF5-23-GlyTCC-2 exerts its tumor-suppressive effects remains the primary focus of our ongoing research.

In conclusion, our comprehensive investigation positions serum tRF5-23-GlyTCC-2 as a robust non-invasive biomarker with dual diagnostic and prognostic value for CRC. We strongly advocate for the concurrent use of tRF5-23-GlyTCC-2 and CEA as a diagnostic panel, representing a clinically translatable strategy to improve CRC detection and risk stratification.

Conclusion

This study identifies tRF5-23-GlyTCC-2 as a novel tsRNA that is lowly expressed in CRC tissues and serum. It demonstrates superior diagnostic value to CEA in distinguishing CRC from controls and polyps, and correlates with advanced stage and poor survival. Functional assays confirm its tumor-suppressive role. Our findings position tRF5-23-GlyTCC-2 not only as a promising non-invasive biomarker for CRC diagnosis and prognosis but also, due to its confirmed growth-inhibitory effect, as a potential therapeutic target, suggesting that restoring its expression may open a novel therapeutic avenue for CRC. Future multicenter validation studies and mechanistic investigations into its downstream pathways, particularly the MAPK signaling pathway, are essential next steps to fully realize its clinical and therapeutic potential.

Data Sharing Statement

The data supporting the findings of this study can be accessed upon reasonable request to the corresponding author.

Ethics Approval and Consent to Participate

Clinical samples were collected after informed consent was obtained from the subjects, and studies involving human subjects were reviewed and approved by the Ethics Committees of the Affiliated Hospital of Nantong University (2019-L053).

Informed consent to participate was obtained from all individual participants included in the study. Each individual's participation was voluntary. The research was performed in accordance with the Declaration of Helsinki and all methods were carried out following relevant guidelines and regulations.

The experiments were approved by the Animal Experiment Ethics Review Form of Nantong University Animal Experiment Center (Approval No. S20241126-026).All procedures were conducted in strict adherence to the ethical principles for animal research outlined in the Basel Declaration and the guidelines set forth by the International Council for Laboratory Animal Science (ICLAS). Every effort was made to minimize the number of animals used and to alleviate their suffering.

Acknowledgments

We appreciate the platform of the Clinical Resource Translational Research Center provided by the Affiliated Hospital of Nantong University for its unwavering support of our investigation. The authors would like to express their sincere gratitude to Lei Shen and Shifang Wang for their valuable assistance and insightful discussions. This work was supported by the Nantong Municipal Health Commission Project (QNZ2023006).

Author Contributions

All authors made a significant contribution to the work reported, whether that is in the conception, study design, execution, acquisition of data, analysis and interpretation, or in all these areas; took part in drafting, revising or critically reviewing the article; gave final approval of the version to be published; have agreed on the journal to which the article has been submitted; and agree to be accountable for all aspects of the work.

Funding

This study was supported by the National Natural Science Foundation of China (81972015), General Project of the Health Commission of Jiangsu Province (H2018074), Nantong Science and Technology Project (JC2019121). This study was supported by grant from Jiangsu Provincial Research Hospital (YJXYY202204-YSB72).

Disclosure

The authors declare no competing interests in this work.

References

1. Li N, Lu B, Luo C, et al. Incidence, mortality, survival, risk factor and screening of colorectal cancer: a comparison among China, Europe, and northern America. *Cancer Lett*. 2021;522:255–268. doi:10.1016/j.canlet.2021.09.034
2. O'Sullivan DE, Sutherland RL, Town S, et al. Risk factors for early-onset colorectal cancer: a systematic review and meta-analysis. *Clin Gastroenterol Hepatol*. 2022;20(6):1229–1240.e5. doi:10.1016/j.cgh.2021.01.037
3. Biller LH, Schrag D. Diagnosis and treatment of metastatic colorectal cancer: a review. *JAMA*. 2021;325(7):669–685. doi:10.1001/jama.2021.0106
4. Zeng H, Chen W, Zheng R, et al. Changing cancer survival in China during 2003-15: a pooled analysis of 17 population-based cancer registries. *Lancet Glob Health*. 2018;6(5):e555–e567. doi:10.1016/s2214-109x(18)30127-x
5. Chen H, Li N, Ren J, et al. Participation and yield of a population-based colorectal cancer screening programme in China. *Gut*. 2019;68 (8):1450–1457. doi:10.1136/gutjnl-2018-317124
6. Liu SC, Zhang H. Early diagnostic strategies for colorectal cancer. *World J Gastroenterol*. 2024;30(33):3818–3822. doi:10.3748/wjg.v30.i33.3818
7. Li C, Zhang D, Pang X, et al. Trajectories of perioperative serum tumor markers and colorectal cancer outcomes: a retrospective, multicenter longitudinal cohort study. *EBioMedicine*. 2021;74:103706. doi:10.1016/j.ebiom.2021.103706
8. Ren G, Li R, Zheng G, et al. Prognostic value of normal levels of preoperative tumor markers in colorectal cancer. *Sci Rep*. 2023;13(1):22830. doi:10.1038/s41598-023-49832-5
9. Li J, Li ZP, Ruan WJ, Wang W. Colorectal cancer screening: the value of early detection and modern challenges. *World J Gastroenterol*. 2024;30 (20):2726–2730. doi:10.3748/wjg.v30.i20.2726
10. Fu M, Gu J, Wang M, et al. Emerging roles of tRNA-derived fragments in cancer. *Mol Cancer*. 2023;22(1):30. doi:10.1186/s12943-023-01739-5
11. Xie Y, Yao L, Yu X, Ruan Y, Li Z, Guo J. Action mechanisms and research methods of tRNA-derived small RNAs. *Signal Transduction Targeted Therap*. 2020;5(1):109. doi:10.1038/s41392-020-00217-4
12. Wang J, Zhu S, Meng N, He Y, Lu R, Yan GR. ncRNA-encoded peptides or proteins and cancer. *Molecular therapy*. 2019;27(10):1718–1725. doi:10.1016/j.ymthe.2019.09.001
13. Zhu L, Ge J, Li T, Shen Y, Guo J. tRNA-derived fragments and tRNA halves: the new players in cancers. *Cancer Lett*. 2019;452:31–37. doi:10.1016/j.canlet.2019.03.012
14. Yang Y, Yan X, Li X, Ma Y, Goel A. Long non-coding RNAs in colorectal cancer: novel oncogenic mechanisms and promising clinical applications. *Cancer Lett*. 2021;504:67–80. doi:10.1016/j.canlet.2021.01.009
15. Du J, Huang T, Zheng Z, Fang S, Deng H, Liu K. Biological function and clinical application prospect of tsRNAs in digestive system biology and pathology. *Cell Communication and Signaling*. 2023;21(1):302. doi:10.1186/s12964-023-01341-8
16. Tao EW, Wang HL, Cheng WY, Liu QQ, Chen YX, Gao QY. A specific tRNA half, 5'tiRNA-His-GTG, responds to hypoxia via the HIF1α/ANG axis and promotes colorectal cancer progression by regulating LATS2. *J Experi Clinl Cancer Res*. 2021;40(1):67. doi:10.1186/s13046-021-01836-7
17. Xu R, Du A, Deng X, et al. tsRNA-GlyGCC promotes colorectal cancer progression and 5-FU resistance by regulating SPIB. *J Experi Clinl Cancer Res*. 2024;43(1):230. doi:10.1186/s13046-024-03132-6
18. Sui S, Wang Z, Cui X, Jin L, Zhu C. The biological behavior of tRNA-derived fragment tRF-Leu-AAG in pancreatic cancer cells. *Bioengineered*. 2022;13(4):10617–10628. doi:10.1080/21655979.2022.2064206
19. Shen Y, Xie Y, Yu X, et al. Clinical diagnostic values of transfer RNA-derived fragment tRF-19-3L7L73JD and its effects on the growth of gastric cancer cells. *J Cancer*. 2021;12(11):3230–3238. doi:10.7150/jca.51567

20. Wang J, Ma G, Ge H, et al. Circulating tRNA-derived small RNAs (tsRNAs) signature for the diagnosis and prognosis of breast cancer. *NPJ Breast Cancer*. 2021;7(1):4. doi:10.1038/s41523-020-00211-7
21. Jin F, Yang L, Wang W, et al. A novel class of tsRNA signatures as biomarkers for diagnosis and prognosis of pancreatic cancer. *Mol Cancer*. 2021;20(1):95. doi:10.1186/s12943-021-01389-5
22. Shao Y, Sun Q, Liu X, Wang P, Wu R, Ma Z. tRF-Leu-CAG promotes cell proliferation and cell cycle in non-small cell lung cancer. *Chem Biol Drug Des*. 2017;90(5):730–738. doi:10.1111/cbdd.12994
23. Gu X, Zhang Y, Huang Y, Ju S. Comprehensive evaluation of serum tRF-17-WS7K092 as a promising biomarker for the diagnosis of gastric cancer. *J Oncol*. 2022;2022:8438726. doi:10.1155/2022/8438726
24. Xue M, Shi M, Xie J, et al. Serum tRNA-derived small RNAs as potential novel diagnostic biomarkers for pancreatic ductal adenocarcinoma. *Am J Cancer Res*. 2021;11(3):837–848.
25. Zhou Y, Hu J, Liu L, et al. Gly-tRF enhances LCSC-like properties and promotes HCC cells migration by targeting NDFIP2. *Can Cell Inter*. 2021;21(1):502. doi:10.1186/s12935-021-02102-8
26. Jin H, Yeom JH, Shin E, et al. 5'-tRNA(Gly(GCC)) halves generated by IRE1α are linked to the ER stress response. *Nat Commun*. 2024;15(1):9273. doi:10.1038/s41467-024-53624-4
27. Wang Q, Huang Q, Ying X, Shen J, Duan S. Unveiling the role of tRNA-derived small RNAs in MAPK signaling pathway: implications for cancer and beyond. *Front Genetics*. 2024;15:1346852. doi:10.3389/fgene.2024.1346852
28. Liu C, Hou X, Mo K, et al. Serum non-coding RNAs for diagnosis and stage of liver fibrosis. *J Clin Lab Analysis*. 2022;36(10):e24658. doi:10.1002/jcla.24658
29. Huang T, Zhao Y, Jiang G, Yang Z. tsRNA: a promising biomarker in breast cancer. *J Cancer*. 2024;15(9):2613–2626. doi:10.7150/jca.93531
30. Chen Q, Zhang X, Shi J, Yan M, Zhou T. Origins and evolving functionalities of tRNA-derived small RNAs. *Trends Biochem Sci*. 2021;46(10):790–804. doi:10.1016/j.tibs.2021.05.001
31. Wu C, Liu D, Zhang L, et al. 5'-tiRNA-Gln inhibits hepatocellular carcinoma progression by repressing translation through the interaction with eukaryotic initiation factor 4A-I. *Front Med*. 2023;17(3):476–492. doi:10.1007/s11684-022-0966-6
32. Cui H, Li H, Wu H, et al. A novel 3'tRNA-derived fragment tRF-Val promotes proliferation and inhibits apoptosis by targeting EEF1A1 in gastric cancer. *Cell Death Dis*. 2022;13(5):471. doi:10.1038/s41419-022-04930-6